Chinese Science Bulletin 2005 Vol. 50 No. 18 2080—2089

Formation history and protolith characteristics of granulite facies metamorphic rock in Central Cathaysia deduced from U-Pb and Lu-Hf isotopic studies of single zircon grains

YU Jinhai[1,2], ZHOU Xinmin[1], Y. S. O'Reilly[2], ZHAO Lei[1], W. L. Griffin[2], WANG Rucheng[1], WANG Lijuan[1] & CHEN Xiaomin[1]

1. State Key Laboratory for Mineral Deposits Research, Department of Earth Sciences, Nanjing University, Nanjing 210093, China;
2. GEMOC ARC National Key Centre, Department of Earth and Planetary Sciences, Macquarie University, Sydney, N.S.W. 2109, Australia

Correspondence should be addressed to Yu Jinhai (email: jhyu@nju.edu.cn)

Abstract **The petrochemical as well as zircon U-Pb and Lu-Hf isotopic studies of granulite facies metamorphic rock from the Taoxi Group in eastern Nanling Range, Central Cathaysia indicate that its protolith is the sedimentary rock with low maturation index. The clastic materials are mostly from middle Neoproterozoic (~736 Ma) granitoid rocks with minor Neoarchaean and Paleoproterozoic rocks. The timing of this Neoproterozoic magmatism is in agreement with the second period of magmatism widespread surrounding the Yangtze Block. Hf isotopic data indicate that the Neoproterozoic granitoids resulted from the recycled Paleoproterozoic mantle-derived crustal materials. The sedimentary rock was deposited in Late Neoproterozoic Era, and carried into low crust in Early Paleozoic. The partial melting of the meta-sedimentary rock took place at about 480 Ma and subsequently granulite facies metamorphism occurred at ca. 443 Ma. The zircons forming during this time interval (Early Paleozoic) show large Hf isotope variations, and their $\varepsilon_{Hf}(t)$ values increase from −13.2 to +2.36 with decreasing age, suggesting the injection of mantle-derived materials during partial melting and metamorphism processes in the Early Paleozoic. Calculation results show that this metamorphic rock, if evolved to Mesozoic, has similar isotopic composition to the nearby Mesozoic high Si peraluminous granites, implying that this kind of granulite facies metamorphic rock is probably the source material of some Mesozoic peraluminous granitoids in eastern Nanling Range.**

Keywords: Granulite, Zircon, U-Pb-Hf isotope, Central Cathaysia.

DOI: 10.1360/982004-808

Precambrian metamorphic basement outcropped in South China Block (SCB) consists mainly of low- to moderate- grade metamorphic rocks, except for those in western part (Shaba area) and northern part (Kongling Group) of the Yangtze Block and central Hainan, which contain some granulite facies metamorphic rocks[1−3]. Other granulites or granulite facies metamorphic rocks in SCB occur as xenoliths in Cenozoic basalts or granites[4−8]. These granulites are dispersive and mostly mafic in chemistry. They cannot completely represent the components of lower crust in SCB, because there are plentiful asynchronous S-type granites in SCB. Recently, we found some granulite facies metamorphic rocks in southwestern Fujian Province[9], Central Cathaysia, which may provide us a window to understand the lower crust component of this area and reveal the genetic link between the nearby granites in different time-type associations and these granulites. This study presents zircon compositions, back-scatter electron (BSE) images, LA-ICPMS U-Pb dating and MC-ICPMS Hf istopic results to characterize the protolith feature and date the formation history of this granulite facies metamorphic rock.

1 Geological background and sample feature

Southwestern Fujian Province is located in eastern Nanling Range, Central Cathaysia (Fig. 1(a)), where different periods of sedimentary or metamorphic rocks and dominant Mesozoic granites (Fig. 1(b)) are distributed. This study sample was collected from Taoxi Group that was thought of as Mesoproterozoic strata[10,11]. Taoxi Group is distributed in Taoxi, Xiangcun, Zhongcun and Zhaoxin of Wuping County, and may be divided into lower and upper units. Lower unit consists mainly of gneisses and leptynites and upper one includes different types of schists. Previous studies confirm the metamorphic grade of these metamorphic rocks only up to lower amphibolite facies[10,11]. But, the recent study shows that some metamorphic rocks in lower unit of Taoxi Group were formed at granulite facies of 750－880℃ and ~1.1GPa[9]. This study sample is a garnet-sillimanite-biotite two-feldspar gneiss collected from lower unit of Taoxi Group near Zhaoxin. This rock contains 71.10% SiO_2, 0.41% TiO_2, 14.64% Al_2O_3, 3.37% FeO+Fe_2O_3, 0.82% MgO, 0.49% CaO, 2.62% Na_2O and 4.27% K_2O with high aluminous saturation index (1.49). The compositions are similar to granitoids, except for slightly higher Al and Ti, implying that the protolith is sandstone with lower maturation index, whose clastic materials were from granitoids. T-P calculations indicate that the peak metamorphism took place at 840－870℃[9].

2 Analytical techniques

The sample was crushed to fine grains with a size of 0.27－0.06 mm, then they were carried out using conventional magnetic and heavy liquid separation technique to obtain zircon-rich heavy sands. 101 zircon grains with different colors and morphology were hand-picked under a Leica binocular microscope, mounted in epoxy disks and

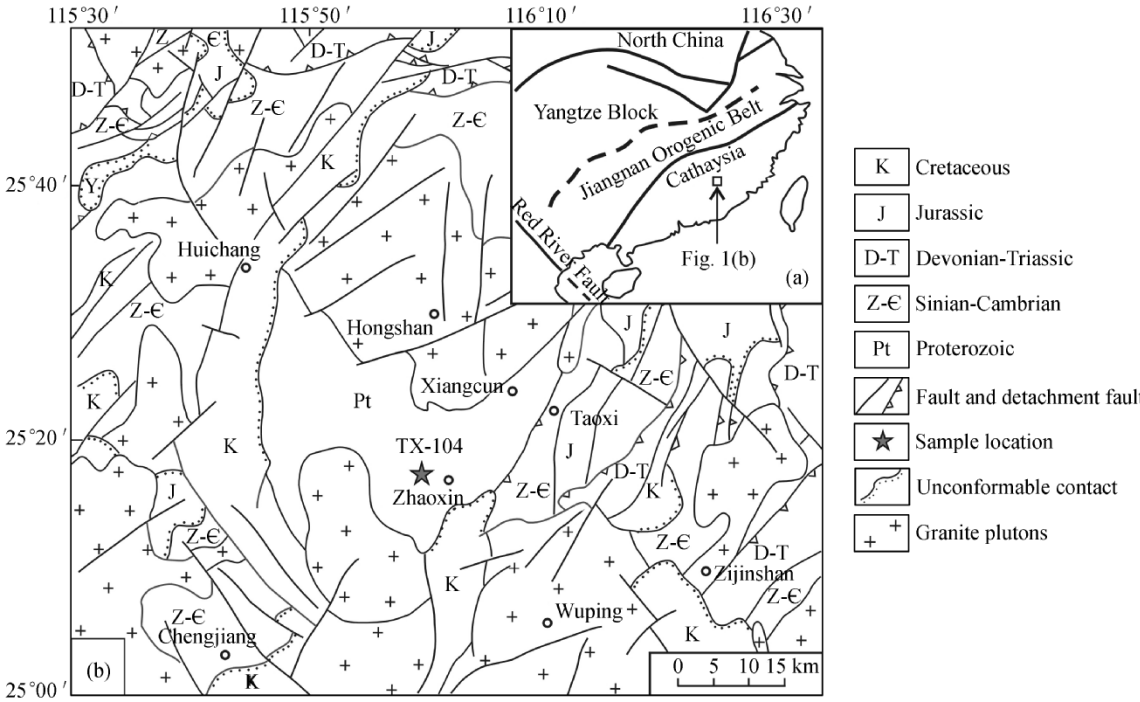

Fig. 1. Sketch geological map showing the study area and sampling location.

polished to core exposure. BSE imaging and composition analyses of each grain were carried out using a CAMECA-SX100 and CAMECA -SX50 electron microprobe respectively, and U-Pb dating and Hf isotope analyses were performed based on BSE images and using an HP 4500 series 300 ICPMS and a Nu Plasma MC ICPMS, respectively. Laser ablation spot diameter is commonly about 40—50 μm in LA-ICPMS U-Pb dating and ~60 μm in MC ICPMS Hf analyses. All above analyses were completed in GEMOC Key Centre of Macquarie University, Australia. The detailed analytical condition and procedure, standard correction and age calculation programs are the same as described by Griffin et al.[12] and Anderson et al.[13].

3 BSE images and compositions of zircons

Zircons in the study sample can be classified into two groups according to their color and shape: The first is colourless to light-pink prismatic zircons with developed (100) face and undeveloped cone; the second is light brown, round to oval-shaped ones with multi-faces or non-faces. Although some grains are round, most of them have strong luster, similar to those metamorphic origin zircons[14,15].

Three types of zircons with different internal structures can be distinguished based on BSE images. Type I is some anhedral or round inherited zircons which exist in the core of most zircon grains (Figs. 2(a)—(d)). They have dark BSE brightness without internal structure, suggesting metamorphic origin or late alteration feature. Type II is present either in mantle or in the core part of zircon grains with euhedral oscillatory growth zoning (Figs. 2(b)—(f)), which should be the magmatic origin or belong to anatectic zircons[15,16]. Type II zircons occurring in the core part (II-c) display dense and homogeneous oscillatory growth zoning (Fig. 2(e)), while Type II zircons in mantle part (II-m) have wider growth zoning (Figs. 2(b)—(d)). Type III zircons forming the outer rim of zircon grains (Fig. 2) have gray and homogeneous BSE image without any zoning, suggesting their metamorphic origin. Most zircon grains with Type II overgrowth are prismatic, while those without Type II are usually oval-shaped (Fig. 2(a)). In fact, the zircons with different sizes do not exhibit essential difference and small grains just have much smaller inherited core.

Electron microprobe analysis results indicate that inherited zircons (Type I) in the core have much lower HfO_2 and $Y_2O_3+ThO_2+UO_2$, and high Th/U ratios. Outer Type III zircons also have homogeneous compositions, but are characterized by high HfO_2, low $Y_2O_3+ThO_2+UO_2$ contents, and the lowest Th/U ratios (Table 1, Fig. 3). Type II-m has large variation of HfO_2 concentrations, of which those zones with bright BSE brightness (II-m-B) have a little lower HfO_2 contents and much higher $Y_2O_3+ThO_2+UO_2$ contents and Th/U ratios than the dark zones (II-m-D) (Table 1, Fig. 3). Type II-c zircons exhibit HfO_2 and $Y_2O_3+ThO_2+UO_2$ contents similar to Type II-m-D, but Th/U ratio is similar to Type II-m-B.

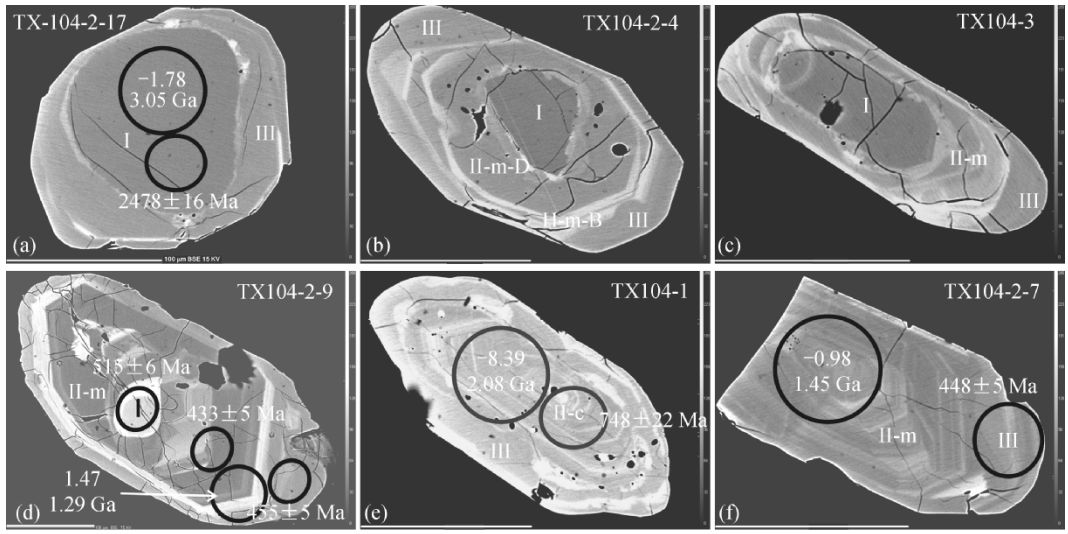

Fig. 2. BSE images of different type zircons from the Taoxi pelitic granulite. Small cycles are the dating positions, and beside them are ages; big cycles are analytical spots of Hf isotope, and within them are $\varepsilon_{Hf}(t)$ values and Hf model ages; scales on left below are all 100 μm.

Table 1 EMP compositions for different type zircons (wt%)

Type	No.	SiO_2	ZrO_2	HfO_2	Y_2O_3	ThO_2	UO_2	Total	Y+Th+U	Y/Hf	Th/U	Th/U*[e](No.)
I	23	31.97	65.71	1.21	0.131	0.022	0.038	99.09	0.191	0.100	0.579	0.556(10)
II-c[a]	7	31.90	65.23	1.57	0.152	0.002	0.040	98.89	0.194	0.090	0.051	0.561(7)
II-m[b]-D[c]	9	32.06	64.87	1.59	0.128	0.021	0.062	98.73	0.211	0.075	0.339	0.317(4)
II-m-B[d]	9	31.69	65.28	1.42	0.251	0.089	0.190	98.92	0.531	0.165	0.468	0.510(5)
III	23	31.75	65.12	1.90	0.112	0.011	0.082	98.98	0.205	0.055	0.134	0.083(5)

a) c—inherited zircon in the core part of zircon grains; b) m—anatectic zircons in the mantle part of zircon grains; c) D—dark growth zoning in BSE images; d) B—bright BSE growth zoning; e) Th/U* is the ratios calculated by LA-ICPMS analysis results, which is more reliable than EMP ratios.

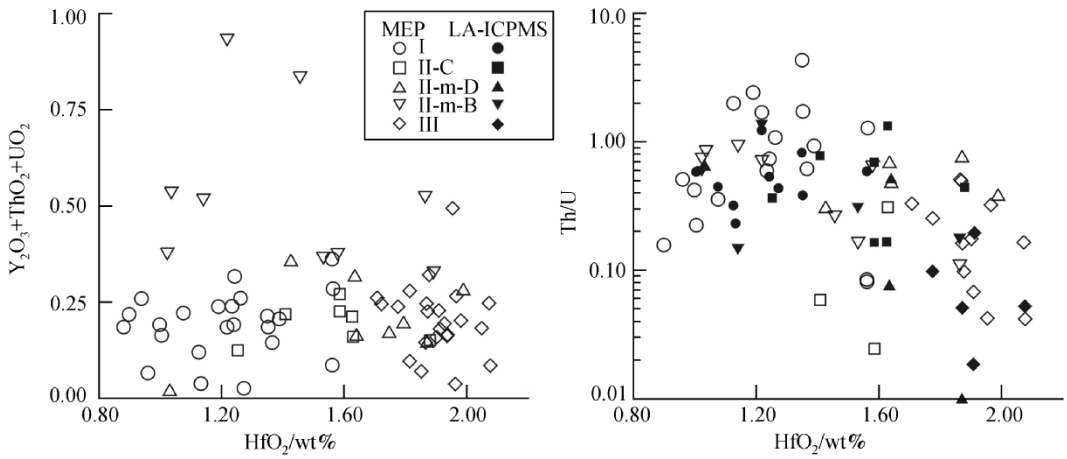

Fig. 3. Composition comparison between different type zircons. Closed symbols indicate LA-ICPMS Th/U ratios.

Generally high Th/U ratios (>0.4) and oscillatory growth zoning are regarded as the features of magmatic origin zircon, whereas zircons with low Th/U ratios (<0.1) and no or weak oscillatory growth zoning are believed to be metamorphic origin[14,17,18]. According to high Th/U ratio, Type I zircons are likely of magmatic origin. The lack of oscillatory growth zoning of these zircons may be accounted for by late thermal event influence. Under the multiphase thermal effect the original composition zoning was likely obliterated through ion diffusion. Very low Th/U ratios and high HfO_2, in combination with no internal structure (see BSE images) indicate that Type III zircons are of metamorphic origin. Type II zircons are all of magmatic origin, but both the structure and dating data

(see below) indicate that II-c and II-m are not the productions of coeval magmatism.

4 Zircon U-Pb dating results

Based on the BSE images and composition characteristics, 37 zircon grains were chosen for LA-ICPMS U-Pb dating. Some large grains are dated both on the core and the rim. As Type III on the rim is generally too narrow (<50 μm), some ages for Type III are probably the results mixing with some Type II-m. In particular, the U-Pb-Th isotope signals of sample TX104-2-12 present obvious step-shaped model as laser ablation, which suggests that laser ablation drills through different types of zircons. Thus these two parts of signals were sampled respectively to calculate their ages. The age obtained from the former section (TX104-2-12q) can reflect the actual age of ablation spot zircon, while the latter age (TX104-2-12h) represents the age of deeper zircon. But, because the signal from the deeper layers may be contaminated by material from the shallower one, the obtained age is a mixed age. In addition, one monazite and two sphene grains were also dated. All analysis results are listed in Table 2.

Dating results show that Type III and II-m zircons have younger ages, and most of them are plotted on or near concordia line in $^{207}Pb/^{235}U-^{206}Pb/^{238}U$ diagram (Fig. 4(a)). The discordances are all <10% (Table 2). Type I and Type II-c zircons have old ages, and majority of them are plotted away from concordia (Fig. 4(b)), suggesting substantive Pb loss. For these zircons $^{207}Pb/^{206}Pb$ ages are closer to actual crystallization age. Thus, the $^{206}Pb/^{238}U$ age values are used to represent the crystallization age of Type III and II-m zircons, whereas the $^{207}Pb/^{206}Pb$ age or the upper intercept age of discordia is accepted for Type I and II-c zircons.

Ages of Type I zircons range from 611 to 2478 Ma, except for grain TX104-2-9c. These analyses cannot construct a discordia in the concordia plot (Fig. 4(b)), implying their different origin. However, three old zircons form a discordia, its upper intercept age is 2523±27 Ma and lower intercept age is 735±45 Ma. The upper intercept age is close to the oldest $^{207}Pb/^{206}Pb$ age of all analysed zircons, implying that the protolith contains less Neoarchean materials. $^{207}Pb/^{206}Pb$ ages of other Type I, ranging from 611 to 737 Ma, are younger than their real crystallization age, because of large discordance (all >10%). Grain TX104-2-9c yields an abnormal young age (495±22 Ma) with good concordant (Table 2), similar to Type II-m. The bright BSE image of this inherited zircon and radiate flaws around it (Fig. 2(d)) suggest that it has high U and Th contents and probably underwent metamictization and volume expanding, because small and U-rich zircon is subject to suffering metamictization and radiogenic Pb loss[18], especially during chemical eluviation and high temperature recrystallization. Consequently, this young age most likely represents the late recrystallization age.

Ages of Type II-c are 594 to 985 Ma and the majority from 683 to 748 Ma, similar to the most of Type I (Table 2). These zircons are also discordant and show radiating Pb loss. Thus the upper intercept age of discordia line is better to reflect real crystallization age. A discordia line formed by these Type II-c zircons and some Type I zircons yield an upper intercept age of 736 Ma (Fig. 4(c)), which is consistent with the lower intercept age of those three old zircons (Fig. 4(b)), suggesting that U-Pb isotopic system of some old inherited zircons was completely reconstituted during ca. 736 Ma magmatism.

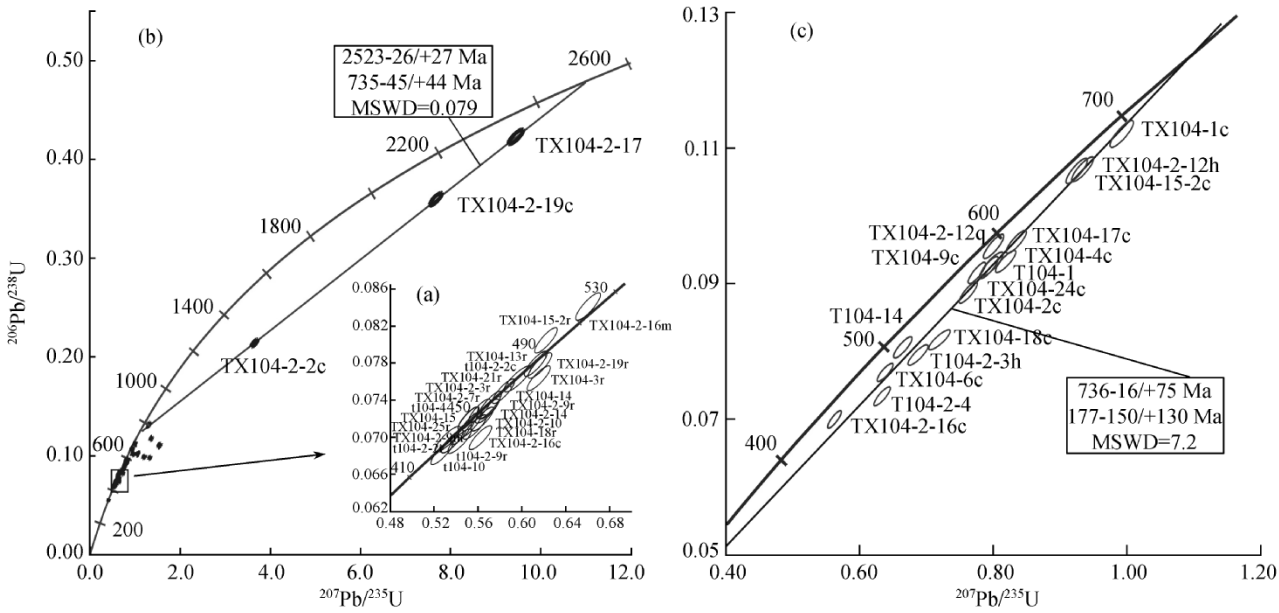

Fig. 4. U-Pb concordia diagram for zircons from the Taoxi granulite.

Table 2 U-Pb dating results for zircons, sphenes and monazite from Taoxi pelitic granulite

Grain number	Zircon type*	Isotopic ratios				Ages			Discordance
		$^{207}Pb/^{235}U$	$^{206}Pb/^{238}U$	$^{207}Pb/^{206}PB$	$^{208}Pb/^{232}Th$	$\frac{^{207}Pb}{^{206}Pb}$	$\frac{^{206}Pb}{^{238}U}$	$\frac{^{207}Pb}{^{235}U}$	
TX104-5c	I	1.32163±0.01491	0.09773±0.00112	0.09813±0.00098	0.03670±0.00038	1589±19	601±7	855±7	−65.1
TX104-6c	I	0.63815±0.00798	0.07690±0.00089	0.06019±0.00069	0.03211±0.00035	611±25	478±5	501±5	−22.6
TX104-9c	I-II	0.77568±0.00870	0.09158±0.00104	0.06144±0.00061	0.03298±0.00031	655±21	565±6	583±5	−14.3
TX104-17c	I	0.83467±0.01009	0.09617±0.00111	0.06294±0.00069	0.03725±0.00036	706±23	592±7	616±6	−16.9
TX104-18c	I	0.71952±0.01073	0.08171±0.00098	0.06386±0.00091	0.03471±0.00040	737±30	506±6	550±6	−32.5
TX104-20c	I	1.04367±0.01373	0.10143±0.00120	0.07463±0.00091	0.03830±0.00037	1058±25	623±7	726±7	−43.2
TX104-2-2c	I	3.64637±0.04676	0.21386±0.00251	0.12367±0.00153	0.08142±0.00095	2010±22	1249±13	1560±10	−41.5
TX104-2-8c	I	0.95102±0.01448	0.10157±0.00129	0.06800±0.00098	0.03616±0.00050	869±30	624±8	679±8	−29.7
TX104-2-17	I	9.44893±0.10699	0.42272±0.00496	0.16215±0.00159	0.12160±0.00110	2478±16	2273±23	2383±10	−9.8
TX104-2-19c	I	7.67138±0.08925	0.35957±0.00427	0.15476±0.00158	0.12430±0.00137	2399±17	1980±20	2193±11	−20.3
t104-2-3	I	0.68740±0.00997	0.07947±0.00100	0.06275±0.00083	0.03670±0.00051	700±28	493±6	531±6	−30.7
t104-2-4	I	0.63362±0.00821	0.07337±0.00093	0.06260±0.00068	0.02728±0.00033	695±23	456±6	498±5	−35.5
t104-2-9c	I	1.53642±0.02126	0.11032±0.00146	0.10094±0.00120	0.04361±0.00053	1642±22	675±9	945±9	−61.9
TX104-2-9c	I	0.65487±0.00745	0.08319±0.00097	0.05711±0.00056	0.02209±0.00022	495±22	515±6	512±5	4.0
TX104-1c	II-c	0.99252±0.01166	0.11210±0.00131	0.06420±0.00066	0.02916±0.00029	748±22	685±8	700±6	−8.9
TX104-2c	II-c	0.76265±0.00906	0.08869±0.00104	0.06238±0.00065	0.03587±0.00036	687±22	548±6	576±5	−21.2
TX104-4c	II-c	0.81878±0.01008	0.09328±0.00108	0.06369±0.00072	0.03035±0.00029	731±24	575±6	607±6	−22.4
TX104-12c	II-c	1.30379±0.01421	0.13142±0.00147	0.07198±0.00071	0.04548±0.00045	985±20	796±8	847±6	−20.5
TX104-15-2c	II-c	0.92507±0.01059	0.10665±0.00123	0.06290±0.00064	0.04089±0.00038	705±22	653±7	665±6	−7.7
TX104-24c	II-c	0.79365±0.00932	0.09238±0.00108	0.06231±0.00065	0.03366±0.00035	685±22	570±6	593±5	−17.6
TX104-2-12q	II-c	0.80066±0.01007	0.09550±0.00117	0.06083±0.00067	0.02957±0.00030	633±24	588±7	597±6	−7.5
TX104-2-12h	II-c	0.93395±0.01091	0.10689±0.00121	0.06338±0.00068	0.03729±0.00036	721±23	655±7	670±6	−9.7
t104-1	II-c	0.79842±0.01096	0.09289±0.00117	0.06227±0.00075	0.03617±0.00042	683±26	573±7	596±6	−16.8
t104-14	II-c	0.66463±0.00912	0.08060±0.00103	0.05972±0.00070	0.02658±0.00034	594±25	500±6	517±6	−16.3
TX104-3r	II	0.61538±0.00703	0.07637±0.00088	0.05844±0.00058	0.03812±0.00047	546±22	474±5	487±4	−13.6
TX104-13r	II-III	0.61265±0.00690	0.07793±0.00090	0.05702±0.00057	0.03189±0.00045	492±22	484±5	485±4	−1.8
TX104-14	II-III	0.57057±0.00714	0.07347±0.00098	0.05635±0.00055	0.03060±0.00045	466±22	457±6	458±5	−2.1
TX104-15-2r	II	0.62204±0.00685	0.08046±0.00091	0.05606±0.00055	0.02392±0.00022	454±21	499±6	491±4	10.1
TX104-25r	II	0.54469±0.00631	0.07044±0.00082	0.05609±0.00057	0.02230±0.00026	456±22	439±5	442±4	−3.9
TX104-2-3r	II-III	0.55144±0.00628	0.07202±0.00083	0.05554±0.00057	0.02330±0.00024	434±23	448±5	446±4	3.4
TX104-2-9m	II	0.53660±0.00657	0.06955±0.00082	0.05597±0.00062	0.02164±0.00021	451±24	433±5	436±4	−4.1
TX104-2-9r	II	0.57083±0.00622	0.07320±0.00081	0.05656±0.00057	0.02204±0.00021	474±22	455±5	459±4	−4.2
TX104-2-10	II	0.56138±0.00653	0.07286±0.00084	0.05589±0.00058	0.02349±0.00022	448±22	453±5	452±4	1.2
TX104-2-14	II	0.56831±0.00698	0.07282±0.00086	0.05661±0.00062	0.02345±0.00023	476±24	453±5	457±5	−5.1
TX104-2-16c	II	0.56226±0.00677	0.06996±0.00085	0.05830±0.00060	0.01480±0.00013	541±23	436±5	453±4	−20.1
TX104-2-16m	II	0.66036±0.00749	0.08410±0.00098	0.05696±0.00056	0.02500±0.00023	489±22	521±6	515±5	6.5
TX104-2-19r	II	0.61656±0.00712	0.07774±0.00091	0.05753±0.00058	0.03642±0.00066	512±22	483±6	488±5	−6.0
t104-2-2c	II	0.59610±0.00811	0.07630±0.00093	0.05666±0.00070	0.03355±0.00058	478±27	474±6	475±5	−0.9
TX104-15	III	0.55309±0.00713	0.07137±0.00095	0.05623±0.00058	0.03113±0.00052	461±23	444±6	447±5	−3.9
TX104-18r	III-II	0.56412±0.00669	0.07196±0.00085	0.05685±0.00059	0.02516±0.00026	485±23	448±5	454±4	−8.0
TX104-21r	III-II	0.58322±0.00672	0.07496±0.00087	0.05643±0.00057	0.02065±0.00024	469±23	466±5	467±4	−0.7
TX104-2-7r	III-II	0.55089±0.00609	0.07203±0.00082	0.05547±0.00055	0.02286±0.00023	431±22	448±5	446±4	4.1
t104-2-2r	III	0.53247±0.00768	0.06982±0.00090	0.05528±0.00070	0.02755±0.00082	424±28	435±5	433±5	2.9
t104-2-9r	III-II	0.54314±0.00709	0.06957±0.00087	0.05662±0.00062	0.02285±0.00037	476±24	434±5	441±5	−9.4
t104-4	III-II	0.55705±0.00697	0.07110±0.00087	0.05681±0.00060	0.02253±0.00026	484±24	443±5	450±5	−8.8
t104-10	III-II	0.52717±0.00671	0.06832±0.00084	0.05595±0.00061	0.02177±0.00027	450±24	426±5	430±5	−5.6
TX104-2-15	Mon	0.58479±0.00666	0.07416±0.00087	0.05720±0.00056	0.02502±0.00022	499±22	461±5	468±4	−7.9
TX104-2-21	Sph	0.64381±0.00728	0.08153±0.00096	0.05728±0.00056	0.02447±0.00022	502±22	505±6	505±5	0.6
t104-7	Sph	0.40896±0.00514	0.05485±0.00069	0.05397±0.00056	0.01804±0.00019	370±23	344±4	348±4	−6.9

*In type column, II-III means that the most of ablated zircons are Type II; III-II means Type III; minus discordance value indicates that analysis result is below the concordia, and positive value is above the concordia; Mon—monazite, Sph—sphene.

Type II-m zircons have low ages, but large variation (433 to 521 Ma). Type III zircons are also young, and overlap the lower age section of Type II-m (Fig. 5, Table 2). Probability and histograms show that Type III and II-m zircons have two age peaks, from 430 to 460 Ma and from 470 to 490 Ma, respectively. The weighted average value of 14 zircons with age of 430 to 460 Ma is 444.8±4.8 Ma, and that of 4 zircons of 470 to 490 Ma is 478.7±5.4 Ma. If only Type III is calculated, the weighted average is 443±10 Ma. In conjunction with their BSE imaging and compositions, the age can be regarded as metamorphism age of this metamorphic rock, otherwise ~480 Ma may reflect the time of a period of magmatism.

Two sphenes and one monazite are all concordant (Table 2), but their ages are different. The monazite and a sphene have similar ages to II-m zircons, but another sphene yields the youngest age (344±4.2 Ma), which likely represents the time of a late and weak thermal disturbing.

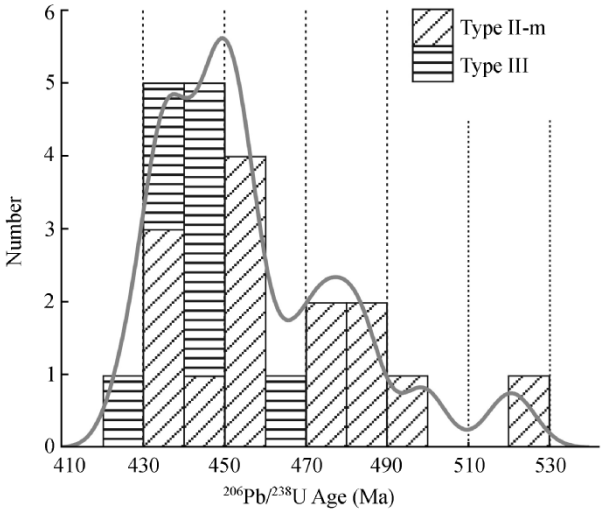

Fig. 5. Ages probability and histogram of Early Paleozoic zircons.

5 Zircon Hf isotopic compositions

Like Sm-Nd isotopic system, Lu/Hf ratio of the residual depleted mantle is increasing during partial melting due to preferential partition of Hf into melt relative to Lu. Thus, $^{176}Hf/^{177}Hf$ ratio of the depleted mantle will increase rapidly with evolution, while that of new crustal component produced from mantle will increase slowly because of low Lu/Hf ratio. Zircon is very suitable for Hf isotopic studies. It has high Hf content and extremely low Lu/Hf ratio, so that correction for radiogenic growth after crystallization can be neglected and analysed $^{176}Hf/^{177}Hf$ ratio can approximately represent the original isotopic ratio[12,19−21]. In addition, zircons can be precisely dated by U-Pb techniques. Thus, a combined study of U-Pb and Lu-Hf isotopic systems can interpret the composition evolution in different periods[19−21].

This study presents Hf isotopic compositions of 18 zircon grains, most of which have been dated. The analytical spot for Hf isotope is close to its dating spot, and shows similar BSE feature to dating part. $\varepsilon_{Hf}(t)$ and T_{DM} calculations for sample TX104-12r and TX104-10r without dating data were carried out using average age of Type III (443 Ma)(Table 3). Analyses results display large variation of $^{176}Hf/^{177}Hf$ ratios among Type I and II-c, which proves again that the protolith of this metamorphic rock contains varied source materials. Three old zircons are different in Hf isotopic compositions. Grains TX104-2-17c and TX104-2-2 have the oldest model age and minus $\varepsilon_{Hf}(t)$ value, suggesting that they derived likely from Mesoarchean crustal materials. Zircon TX104-2-19c exhibits the same model age as its U-Pb age, and positive $\varepsilon_{Hf}(t)$ value similar to depleted mantle, suggesting that it crystallized directly from early Paleoproterozoic mantle-derived magma. Neoproterozoic zircons with vey low $\varepsilon_{Hf}(t)$ value display two model age groups, 2.31—2.41 Ga and 2.04—2.07 Ga, respectively. The first group zircons are on evolution trend of zircon TX104-2-19c assuming that its host rock has average crustal composition (Fig. 6(a)), indicating that the original magma of these zircons originated probably from Paleoproterozoic mantle-derived compositions. The parental magma of the second group zircons may be generated by partial melting from middle Paleoproterozoic mantle-derived crustal materials.

Although Types II-m and III exhibit similar age, their $^{176}Hf/^{177}Hf$ ratios are variable. Their $\varepsilon_{Hf}(t)$ values range from −13.2 to +2.36, and model ages (T_{DM}) from 2.19 to 1.24 Ga. It can be observed from Fig. 6(b) that $\varepsilon_{Hf}(t)$ displays negative correlation with time. This change trend is different from crust evolution and depleted mantle one. Combined with the magmatic genesis of Type II zircons and model age variation, it can be concluded that the $\varepsilon_{Hf}(t)$ change was probably caused by incessant importing of juvenile mantle-derived liquids; that is, Early Paleozoic produced magma was greatly contaminated by juvenile mantle-derived melt or fluid during the melting and subsequent crystallization. In this process the inherited zircons cannot be affected and early formed zircons, such as TX104-2-14 and TX104-21, were influenced more weakly. However, late zircons and later rock-forming minerals were affected by more and more mantle-derived materials. Consequently overgrowth zircons formed by the decomposing of some Zr-, Hf-bearing rock-forming minerals during granulite facies metamorphism at ca. 443 Ma would inherit more mantle composition characteristics.

6 Discussion and conclusion

6.1 Granulite formation history

BSE images and chemical compositions of zircons indicate that there are at least three types of zircons in the Taoxi granulite facies metamorphic rock. Types I and II-c

Table 3 Hf isotopic compositions for zircons from the Taoxi granulite

Sample	$^{176}Hf/^{177}Hf$	$^{176}Lu/^{177}Hf$	$^{176}Yb/^{177}Hf$	Ages(Ma)	T_{DM}	$\varepsilon_{Hf}(t)$	Type
TX104-10r	0.282338±0.000014	0.001675±0.000039	0.043183	443	1.74	−5.78±0.50	II-III
TX104-12r	0.282276±0.000020	0.001689±0.000044	0.044108	443	1.87	−7.98±0.71	II-III
TX104-21r	0.282236±0.000015	0.000668±0.000009	0.018192	466	1.92	−8.57±0.53	III-II
TX104-2-3r	0.282358±0.000016	0.002669±0.000070	0.073171	448	1.71	−5.26±0.57	II-III
TX104-2-7c	0.282475±0.000023	0.002214±0.000014	0.057777	448	1.45	−0.98±0.81	II-III
TX104-2-9	0.282539±0.000024	0.000518±0.000011	0.014024	433	1.29	1.47±0.85	III-II
TX104-2-16c	0.282574±0.000035	0.001888±0.000029	0.053129	436	1.24	2.36±1.24	II-III
TX104-2-10c	0.282531±0.000021	0.001442±0.000008	0.039786	453	1.31	1.35±0.74	II-m
TX104-2-14	0.282118±0.000015	0.001056±0.000005	0.028095	453	2.19	−13.16±0.53	II-m
TX104-1c	0.282107±0.000022	0.001034±0.000005	0.025134	748	2.04	−6.99±0.78	II-c
TX104-15-2c	0.282107±0.000017	0.001037±0.000016	0.027974	705	2.07	−7.95±0.60	II-c
TX104-12c	0.281882±0.000014	0.001596±0.000046	0.042842	985	2.41	−10.04±0.50	II-c
TX104-6c	0.282022±0.000026	0.001396±0.000038	0.036492	611	2.31	−13.21±0.92	I-II
TX104-2-8c	0.282064±0.000026	0.001188±0.000033	0.033501	869	2.07	−5.91±0.92	I
TX104-18c	0.281938±0.000018	0.001579±0.000061	0.040587	737	2.42	−13.50±0.64	I
TX104-20c	0.281907±0.000027	0.001844±0.000019	0.046712	1058	2.32	−7.73±0.96	I
TX104-2-19c	0.281421±0.000041	0.000297±0.000002	0.007673	2399	2.45	7.41±1.46	I
TX104-2-2c	0.281344±0.000024	0.000505±0.000005	0.016218	2010	2.87	−4.79±0.85	I
TX104-2-17c	0.281115±0.000025	0.000401±0.000001	0.010221	2478	3.05	−1.78±0.89	I

Present whole earth average: $^{176}Hf/^{177}Hf = 0.282772$, $^{176}Lu/^{177}Hf = 0.0332$, $\lambda(^{176}Lu)=1.93\times10^{-11}yr^{-1}$; T_{MD} (Ga) values are calculated by two-step model assuming that $^{176}Lu/^{177}Hf$ of crust is 0.015[12].

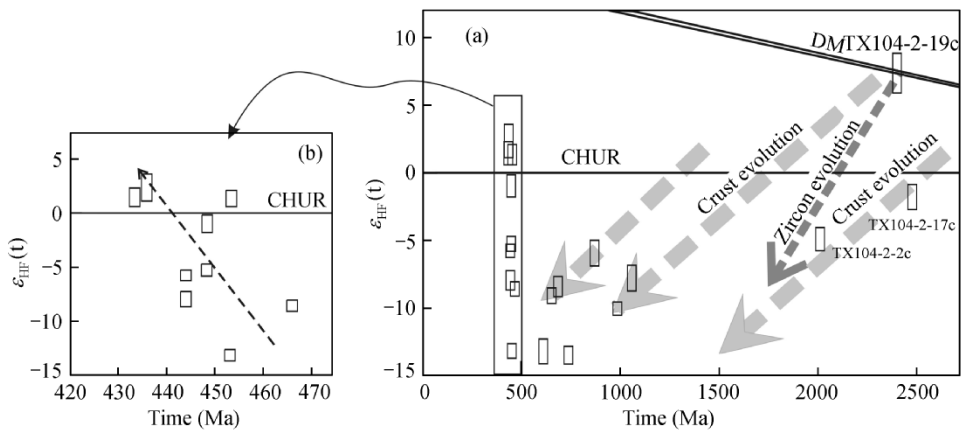

Fig. 6. $\varepsilon_{Hf}(t)-t$ plots for different type zircons. Symbol highness shows the $\varepsilon_{Hf}(t)$ variation range calculated by analytical errors.

zircons in the core belong to source components and have different crystallization ages and Hf isotopic compositions, indicating that the protolith is composed of different source materials. These protolith zircons mostly formed at Neoproterozoic (~736 Ma), and a few crystallized at Neoarchean and Paleoproterozoic. Considering that late partial melting and metamorphism took place after 520 Ma, Taoxi Group should belong to Late Neoproterozoic strata, and be not Mesproterozoic as formerly reported[10,11].

Neoproterozoic magmatism was very intense in South China, especially along the margin of the Yangtze Block[22−24], which was thought to be closely related with superplume that led to the breakup of Rodinia supercontinent[23−27]. Statistic analyses of recently reported zircon U-Pb dating results show that Neoproterozoic magmatism in South China took place in two periods, 825 to 797 Ma and 766 to 702 Ma, respectively. However, these two periods of magmatism were rarely reported in Cathaysia Block in previous studies. Recently, according to SHRIMP U-Pb zircon age (818±9 Ma), Li et al.[27] thought that the Mamianshan bimodal volcanic rocks in northwestern Fujian Province were the production of Neoproterozoic

rifting. Although this study sample is paragneiss, both chemical composition and euhedral Type II-c zircons indicate that main source components of the protolith came from vicinal regions. It is suggested that intense Neoproterozoic magmatism also occurred in the study area or nearby. Combined with the present authors' unpublished dating results for detrital zircons in meta-sediments from eastern and northern Guangzhou Province and southern Jiangxi Province, we believe that Neoproterozoic magmatism was also extensive in Cathaysia Block. But in subsequent geological history Cathaysia Block experienced much strong tectonic and magmatism, and consequently the most of these Neoproterozoic rocks were probably reworked.

Type III zircons show chemical features and internal structures of metamorphic origin. Very low Y_2O_3 (same as HREE) concentrations indicate that they crystallized at the same time with metamorphic garnets, i.e. Type III zircon overgrowth occurred during the peak metamorphism. Therefore 443±10 Ma should reflect peak granulite facies metamorphism time, which is consistent with many Caledonian granites and migmatites widespread in the Cathaysia Block[28,29]. The ages of Type II-m with magmatic characters are also quite young, and even some grains are as young as the metamorphic age. Evidently, magmatism and metamorphism are unlikely to occur synchronously. Moreover, wide age spectrum of Type II-m (interval ~88 Ma) also indicates that they crystallized unlikely from single magmatism. Consequently, we think that those Type II-m zircons with similar age to the metamorphism are most likely influenced by granulite facies metamorphism, which resulted in radiogenic Pb loss and restarted U-Pb isotopic system. Because metamorphism is very close to magmatism, less radiogenic Pb loss cannot make these magmatic zircons deviate obviously from concordia. Therefore, 478.7±5.4 Ma may reflect the age of this partial melting event.

6.2 Composition evolution deduced from U-Pb-Hf isotope

Al-rich and chemical compositions similar to granitoids suggest that the protolith of the granulite is feldspathic sandstone with low maturation index, which resulted likely from Neoproterozoic granite or rhyolite through weathering, short-distance transportation and precipitation. The protolith also includes a few Neoarchean and Paleoproterozoic compositions. Mesoarchean and Neoarchean Hf model age and different $\varepsilon_{Hf}(t)$ of the old zircons indicate that some grains crystallized from the melt generated by partial melting from older mantle-derived rocks, and others formed directly from juvenile mantle-derived magma. However, the rocks formed prior to Paleoproterozoic have not been found in the Cathaysia Block, and all old ages obtained before were determined from detrital zircons[30,31]. Based on the oval shape of three oldest inherited zircons (Fig. 2(a)), they may be accounted for experiencing multiple recycling of old magmatic products in the study area, or coming from remote other blocks, such as the Yangtze Block or the Australia Block.

Low $\varepsilon_{Hf}(t)$ and Paleoproterozoic model age indicate that these Neoproterozoic zircons crystallized probably from the magma originating (by partial melting) from the recycled Paleoproterozoic mantle-derived crustal materials (Fig. 6(a)). These zircons are either detrital (Type I) or euhedral (Type II-c), reflecting that they came from the widespread Neoproterozoic rocks with different origin. However, the Mamianshan bimodal volcanic rocks in northwestern Fujian Province have high $\varepsilon_{Nd}(t)$ values (−4.4 to +3.3)[27], which suggests the injection of the mantle-derived basaltic magma and the mixing with crust materials. Therefore the juvenile mantle-derived magmatism also existed in the Cathaysia Block, though Neoproterozoic magmatism was involved mainly with the recycled old crustal materials.

Peraluminous characteristic and presence of many inherited zircons and relict kyanite[9] indicate that Early Paleozoic partial melting did not make complete separation of melt from relicts, which means that melt still contains plentiful relicts. However, the afflux of juvenile mantle-derived melts or fluids largely altered the compositions of the metamorphic rock, especially in isotopic compositions. Before the injection of Early Paleozoic mantle-derived liquids, the rock was very low in Hf isotopic composition and has Early Paleoproterozoic model age (2.3 to 2.4 Ga). This rock should have $\varepsilon_{Hf}(t)$ value of less than −12 if it evolved to 450 Ma (Fig. 6(a)). However, due to the injection of mantle-derived compositions, $^{176}Hf/^{177}Hf$ ratio and $\varepsilon_{Hf}(t)$ value were greatly increased up to more than −8.0. Because the refractory components, such as zircon, only occupied a few proportions, Hf isotopic composition of Early Paleozoic zircons may represent approximately the isotopic characteristic of the whole rock. Average calculations of Hf isotopic composition of these zircons yield $^{176}Hf/^{177}Hf$ of 0.282383, ε_{Hf}(450Ma) of −4.0 and model age of 1.64 Ga, respectively. According to the formula $\varepsilon_{Hf} = 1.36\times\varepsilon_{Nd} + 3$, proposed by Vervoort[32], ε_{Nd}(450Ma) is calculated to be −5.15, which is similar to some Caledonian granites and migmatites in South China[33−36]. If the rocks with this isotopic composition and average crustal $^{176}Lu/^{177}Hf$ ratios (0.015) evolved to Early Yanshanian (160—170 Ma), the $\varepsilon_{Hf}(t)$ value will be −7.5 to −7.6, corresponding with $\varepsilon_{Nd}(t)$ of −7.7 to −7.8. These calculations indicate that the partial melting of this kind of rock in Early Yanshanian would generate the granitoids with slightly higher $\varepsilon_{Hf}(t)$ [and $\varepsilon_{Nd}(t)$] values and Mesoproterozoic model age, which is consistent with some Mesozoic peraluminous high-Si granites in the east-

ern Nanling Range[37−39] if considering the influence of relict components, e.g. inherited zircon. Consequently, this granulite facies metamorphic rock is probably the protolith of some peraluminous granites in Nanling Range area.

According to the model ages of whole rocks, some researchers thought that some granites in South China resulted from the recycled Mesoproterozoic crustal materials by partial melting[34,35,40]. However, U-Pb-Hf isotopic studies of single zircons show that there was not intense Mesoproterozoic mantle-derived magmatism in the study region. Therefore the above inference may not be right. Mesoproterozoic model age is likely the results of the mixture of asynchronous mantle-derived compositions.

Early Paleozoic event (Caledonian) was regarded as a folding orogeny before, and a great number of migmatites in South China were believed to be the results of this tectono-thermal event[29,36,41]. This study indicates that Caledonian orogeny is also extremely intense in eastern Nanling Range (southern Wuyi Mountain), which caused the subduction of Late Neoproterozoic Taoxi Group toward the lower crust. In the deep lower crust, the Taoxi Group rocks experienced not only the partial melting and high-grade metamorphism, but also the contamination by contemporaneous mantle-derived compositions. Consequently, the crust-mantle interaction is an important aspect of Caledonian event. In other words, extensive granitic magmatism and metamorphism are probably correlated with the underplating of mantle-derived liquids. This periodic mantle contribution to crust component was generally neglected in the previous studies[42]. However, the occurrence of many Caledonian granites and this metamorphic rock with the above isotopic characteristic [high $\varepsilon_{Hf}(t)$ and $\varepsilon_{Nd}(t)$ values and Mesoproterozoic model age] and coeval mafic magmatism in nearby areas[43,44] indicate that Early Paleozoic mantle-derived magmatism is an important contribution to the Cathaysia Block.

Acknowledgements We thank Chen Zelin and Xie Lei for cheerful assistance to field sampling, Mr. Norman and Ms. Suzie in GEMOC National Key Center for expert assistance to analytical work, and two anonymous reviewers for their constructive comments that help improving the manuscript. This work was funded by the National Natural Science Foundation of China (Grant Nos. 40372087 and 40132010) and National Innovation Group Foundation of China (Grant No. 40221301). This is contribution No. 401 from the ARC National Key Centre for the Geochemical Evolution and Metallogeny of Continents.

References

1. Lu Huaipeng, Xu Shijin, Wang Rucheng et al., Metamorphism of the Shaba granulites in western Sichuan, Journal of Nanjing University (Nature Sciences), 1999, 35(3): 296−302.
2. Gao Shan, Qiu Yunmin, Ling Wenli et al., SHRIMP single zircon U-Pb dating of the Kongling high-grade metamorphic terrain: Evidence for >3.2Ga old continental crust in the Yangtze craton, Science in China, Ser. D, 2001, 44: 326−335.
3. Zhang Yeming, Zhang Renjie, Hu Ning et al., High grade metamorphic complexes in middle Hainan Island: Ages of the Pb-Pb single zircons and their geological significance, Acta Geoscientia Sinica, 1999, 20(3): 284−288.
4. Xu Xisheng, Zhou Xinmin, The xenoliths from Qilin Cenozoic basaltic pipe, Guangdong, Acta Petrologica Sinica, 1995, 11(4): 441−448.
5. Yu Jinhai, Zhao Lei, Xu Xisheng, Discovery and implications of granulite facies xenoliths from some Cenozoic basalts, SE China, Geological Journal of China Universities, 2002, 8(3): 280−292.
6. Yu Jinhai, Xu Xisheng, O'Reilly, S. Y. et al., Granulite xenoliths from Cenozoic basalts in SE China provide geochemical fingerprints to distinguish lower crust terranes from the North and South China tectonic blocks, Lithos, 2003, 67: 77−102.
7. Chen Bin, Zhang Yuxun, The petrology and petrogeneses of Yunlu charnockite and its granulite inclusion in west Guangdong, South China, Acta Petrologica Sinica, 1994, 10(2): 139−149.
8. Du Yangsong, Collerson, K. D., Zhao Jianxin et al., Characteristics and petrogenesis of granulite enclaves in S-type granites in the junction of Guangdong and Guangxi provinces, Acta Petrologica Sinica, 1999, 15(2): 309−314.
9. Yu Jinhai, Zhou Xinmin, Zhao Lei et al., Discovery and implications of granulite facies metamorphic rocks in the eastern Nanling, China, Acta Petrologica Sinica, 2003, 19(3): 461−467.
10. Ma Jinqing, Wang Wenteng, Basic characteristics and stratigraphic-time basis of middle and lower Proterozoic metamorphic rocks in the Yongding area of Fujian Province, Geology of Fujian, 1993, 12(4): 268−279.
11. Zhuang Jianmin, Huang Quanzhen, Deng Benzong et al., Strata subdivision and petrology of Precambrian metamorphic rocks in Fujian, Xiamen: Xiamen University Press, 2000, 80−90.
12. Griffin, W. L., Wang Xiang, Jackson, S. E. et al., Zircon chemistry and magma mixing, SE China: In-situ analysis of Hf isotopes, Tonglu and Pingtan igneous complexes, Lithos, 2002, 61: 237−269.
13. Andersen, T., Griffin, W. L., Jackson, S. E. et al., Mid-Proterozoic magmatic arc evolution at the southwest margin of the Baltic Shield, Lithos, 2004, 73: 289−318.
14. Wu Yuanbao, Zheng Yongfei, Genesis of zircon and its constraints on interpretation of U-Pb age, Chinese Science Bulletin, 2004, 49(15): 1554−1569.
15. Jian Ping, Cheng Yuqi, Liu Dunyi, Petrographical study of metamorphic zircon: basic roles in interpretation of U-Pb age of high grade metamorphic rocks, Earth Science Frontiers, 2001, 8: 193−191.
16. Keay, S., Lister, G., Buick, I., The timing of partial melting, Barrovian metamorphism and granite intrusion in the Naxos metamorphic core complex, Cyclades, Aegean Sea, Greece, Tectonophysics, 2001, 342: 275−312.
17. Vavra, G., Schmid, R., Gebauer, D., Internal morphology, habit and U-Th-Pb microanalysis of amphibole to granulite facies zircon: geochronology of the Ivren Zone (Southern Alps), Contrib. Mineral. Petrol., 1999, 134: 380−404.

18. Chen Daogong, Isachsen, C., Zhi Xiachen et al., Zircon U/Pb ages for gneiss from Qianshan, Anhui, Chinese Science Bulletin, 2000, 45(8): 764－767.
19. Amelin, Y., Lee, D. C., Halliday, A. N. et al., Nature of the earth's earliest crust from hafnium isotopes in single detrital zircons, Nature, 1999, 399: 252－255.
20. Bodet, F., Scharer, U., Evolution of the SE-Asian continent from U-Pb and Hf isotopes in single grains of zircon and baddeleyite from large rivers, Geochim, Cosmochim. Acta, 2000, 64: 2067－2091.
21. Samson, S. D., D'Lemos, R. S., Blichert-Toft, J. et al., U-Pb geochronology and Hf-Nd isotope compositions of the oldest Neoproterozoic crust within the Cadomian orogen: new evidence for a unique juvenile terrane, Earth Planet Sci. Lett., 2003, 208: 165－180.
22. Li, X. H., U-Pb zircon ages of granites from the southern margin of the Yanhtze Block: Timing of Neoproterozoic Jinning orogeny in SE China and implications of for Rodinia assembly, Precam. Res., 1999, 97: 43－57.
23. Li, X. H., Li, Z. X., Zhou, H. W. et al., U-Pb zircon geochronology, geochemistry and Nd isotopic of Neoproterozoic bimodal volcanic rocks in the Kangdian rift of South China: implications for the initial rifting of Rodinia, Precam. Res., 2002, 113: 135－154.
24. Li, Z. X., Li, X. H., Kinny, P. D. et al., The breakup of Rodinia: Did it start with a mantle plume beneath South China?, Earth Planet Sci. Lett., 1999, 173: 171－181.
25. Li, X. H., Li, Z. X., Ge, W. et al., Neoproterozoic granitoids in South China: crustal melting above a mantle plume at ca. 825 Ma?, Precam. Res., 2003, 122: 45－83.
26. Li, Z. X., Li, X. H., Kinny, P. D. et al., Geochronology of Neoproterozoic syn-rift magmatism in the Yangtze Craton, South China and correlations with other continents: evidence for a mantle superplume that broke up Rodinia, Precam. Res., 2003, 122: 85－109.
27. Li, W. X., Li, X. H., Li, Z. X., Neoproterozoic bimodal magmatism in the Cathaysia Block of South China and its tectonic significance, Precam. Res., 2005, 136: 51－66.
28. Yuan Zhengxin, Zhong Guofang, Xie Yanbao et al., A new recognition on spacial-temporal characteristics of the Caledonian orogeny happened in South China, Geology and Mineral Resources of South China, 1997, (4): 19－25.
29. Wang Jianghai, Tu Xianglin, Sun Dazhong, U-Pb dating of anatectic migmatites at Gaozhou in the Yunkai Block, western Guangdong, China, Geochemica, 1999, 28: 231－238.
30. Zheng, Y. F., Neoproterozoic magmatic activity and global change, Chinese Science Bulletin, 2003, 48(16): 1639－1656.
31. Gan Xiaochun, Zhao Fengqing, Jin Wenshan et al., The U-Pb ages of early Proterozoic-Archean zircons captured by igneous rocks in southern China, Geochimica, 1996, 25(2): 112－120.
32. Vervoort, J. D., Patchett, P. J., Blichert-Toft, J. et al., Relationships between Lu-Hf and Sm-Nd isotopic systems in the global sedimentary system, Earth Planet Sci. Lett., 1999, 168: 79－99.
33. Huang Xuan, Depaolo, D. J., Study of sources of Paleozoic granitoids and the basement of South China by means of Nd-Sr isotope, Acta Petrologica Sinica, 1989, 5(1): 28－36.
34. Wang Dezi, Shen Weizhou, Genesis of granitoids and crustal evolution in southeast China, Earth Science Frontiers, 2003, 10(3): 209－220.
35. Shen Weizhou, Ling Hongfei, Li Wuxian et al., Study on the Nd-Sr isotopic compositions of granitoids in SE China, Geological Journal of China Universities, 1999, 5: 22－32.
36. Hu Gongren, Yu Ruilian, Liu Congqiang, Petrology and isotopic geochemistry of Jinxi-Nancheng migmatites and granites, Jiangxi Province, Acta Petrologica Et Mineralogica, 2001, 20: 102－110.
37. Shen Weizhou, Wang Dezi, Xie Yonglin et al., Geochemical characteristics and material sources of the Qianlishan composite granite body, Hunan Province, Acta Petrologica Et Mineralogica, 1995, 14(3): 193－202.
38. Shen Weizhou, Ling Hingfei, Li Wuxian et al., Crust evolution in southeast China: evidence from Nd model ages of granitoids, Science in China, Ser. D, 2000, 43(1): 36－49.
39. Zhao Lei, Yu Jinhai, Xie Lei, Geochemistry and origin of the Hongshan topaz-bearing leucogranites in southwesten Fujian Province, Geochimica, 2004, 33: 372－386.
40. Hong Dawei, Xie Xilin, Zhang Jisheng, An exploration on the composition, nature and evolution of mid-lower crust in South China based on the Sm-Nd isotopic data of granites, Geological Journal of China Universities, 1999, 5: 361－371.
41. Huang Biao, Sun Mingzhi, Wu Shaoxing et al., Studies on genesis and characters of Caledonian migmatites in middle Wuyi Mountains, Acta Petrologica Sinica, 1994, 10(4): 427－439.
42. Shen Weizhou, Yu Jinhai, Zhao Lei et al., Nd isotopic characteristic of post-Archean sediments from the Eastern Nanling Range: Evidence for crustal evolution, Chinese Science Bulletin, 2003, 48(16): 1679－1685.
43. Yang Shufeng, Chen Hanlin, Wu Guanghai et al., Discovery of Early Paleozoic island-arc volcanic rocks in northern part of Fujian province and the significance for tectonic study, Scientia Geological Sinica, 1995, 30: 105－116.
44. Ren Shengli, Li Jiliang, Zhou Xinhua et al., Petrochemistry and mineral chemistry studies on metamorphic ultramafic rocks in Yanghou area, Zhenghe County, Fujian Province, China, Geochimica, 1997, 26(4): 13－23.

(Received February 2, 2005; accepted May 16, 2005)